Journal of Molecular Structure 1217 (2020) 128449

Contents lists available at ScienceDirect

Journal of Molecular Structure

journal homepage: http://www.elsevier.com/locate/molstruc

Experimental and theoretical studies on monoazo dye including diphenylamine and *N*-methyldiphenylamine derivatives

Tuğçe Aksungur [a], Fatma Erol, Assit.Prof.Dr. [b], Nurgül Seferoğlu, Prof.Dr. [c], Zeynel Seferoğlu, Prof.Dr. [a, *]

[a] Department of Chemistry, Gazi University, Ankara, 06560, Turkey
[b] Technical Sciences Vocational School, Gazi University, Ankara, 06374, Turkey
[c] Department of Advanced Technologies, Graduate School of Natural and Applied Sciences, Gazi University, Ankara, 06560, Turkey

ARTICLE INFO

Article history:
Received 4 April 2020
Received in revised form
10 May 2020
Accepted 13 May 2020
Available online 18 May 2020

Keywords:
Azo dyes
Push-pull chromophores
Proton sensitive dyes
Low pH sensor
NLO
DFT

ABSTRACT

In this manuscript, two series of azo dyes preparing by coupling diphenylamine and *N*-methyl diphenylamine and diazotized substituted anilines bearing various substituents were designed and synthesized. These azo dyes were characterized by spectroscopic techniques such as $^{1}H/^{13}C$ NMR and HRMS or LCMS. Photophysical, NLO and protonation properties were investigated by experimentally and theoretically. The absorption maxima were observed in long wavelength in DMSO. The most stable tautomeric form of dyes which have tautomeric forms, were determined using model compounds. The results showed that the azo dyes are stable in azo form in all solvents used. For the usability as optic dye of the synthesized dyes, thermal property of all dyes was also determined. The all compounds are thermally stable and T_d values are bigger than 220 °C.

1. Introduction

Azo dyes are among the most important classes of synthetic dyes due to the fact that they are synthesized easily and have broad color spectrum [1]. Although a number of azo dyes have been reported to be poisonous, a lot of them are being used in drugs and food [2]. Azo dyes are known essential compounds [3,4] and are applicable not only for dyeing [5–7] but also for high-technology applications [7–9]. For the fact that they are organic dyes bearing auxochromes such as amino, alkylamino, dialkylamino, hydroxy, alkoxy, and nitro groups, they are usually solid. These auxochromes can induce strong polarity into a molecule and then increase its intermolecular interactions. Additionally, they also make the dye molecule often large and having π-electrons to exhibit strong disperse forces and π-π interactions. (see Figs. 9 and 10)

Azo-functionalized dyes appended with aromatic heterocyclic moieties [10] have shown increasing attention recently as a result of having varieties of applications in metallochromic indicators [11], optical data storage [12], non-linear optics (NLO) [13], and dye-sensitized solar cells (DSSC) [14]. Aromatic azo derivatives, especially those having intramolecular D-π-A charge-transfer chromophores have exhibited excellent photophysical properties [15–17] because they possess extensive π-systems delocalized between the acceptor and donor units across the azo linkage. Moreover, azo dyes have different applications that range from textile dyeing [18], leather dyeing [19], coloring of plastics and polymer [20] to advanced usages such as liquid crystal displays [21], in biological and medical investigations and advanced application in organic synthesis [22].

In recent years, a great effort has been exerted in the synthesis of new materials with large second-order optical non-linearity as a result of their potential usage in applications such as high bit rate long-distance optical communications, and more generally, for optical information processing [23]. Again, due to their advanced functional properties such as optical storage capacity, optical switching, holography and non-linear optical (NLO) properties, molecules with azo moieties show promising capability as photoactive materials [24–26]. NLO materials have attracted great interest among several researchers at present time due to their significant applications in optoelectronic and photonic

* Corresponding author.
E-mail addresses: nurguls@gazi.edu.tr (N. Seferoğlu), znseferoglu@gazi.edu.tr (Z. Seferoğlu).

https://doi.org/10.1016/j.molstruc.2020.128449
0022-2860/

technologies [27–30]. The principal advantages of organic second-order NLO molecules are their high NLO activity, chemical stability, and are easily processed [31]. Organic molecules that possess large NLO responses are needed for lots of applicability ranging from the development of photonic devices [32] to biological or medical applications [33].

In our previous study [34], diphenylamine based azo dye named as ((*E*)-1-(4-((4-(phenylamino)phenyl)diazenyl)phenyl)ethanone, **DPA** was synthesized and investigated its photophysical and NLO properties. This compound showed good photophysical and NLO properties therefore, it can be a good candidate for optic application as NLO dyes. Thus, in this current study, two new additional series of azo dyes bearing various substituents and coupling components designed and synthesized. Photophysical, NLO and protonation properties of the compounds were investigated by using experimentally and theoretically. In first series (**I-VI**), the compounds can be shown azo-hydrazone tautomerism due to the transfer of hydrogen of the −NH of diphenylamine. For the determination of the most stable tautomeric form of the first serie of compounds, the second serie of compounds (**I′-VI′**) having no tautomeric forms because of blocking NH proton by methyl substituted were used as model compounds. However, the thermal property of the compounds was determined to estimate their usability as an optical dye.

2. Experimental

2.1. Materials and physical measurements

All commercially available chemicals were reagent grade and used without further purification. Thin-layer chromatography (TLC) was used for monitoring the reactions using precoated silica gel 60 F254 plates. NMR spectra were measured on Bruker Avance 300 (^{1}H: 300 MHz, ^{13}C: 75 MHz) spectrometers at 25 °C (298 K). Chemical shifts (δ) are given in parts per million (ppm) using the residue solvent peaks as a reference relative to TMS. Coupling constants (J) are given in hertz (Hz). Signals are abbreviated as follows: broad. br; singlet. s; doublet. d; doublet-doublet. dd; doublet-triplet dt; triplet. t; multiplet. m. High-resolution mass (HRMS) spectra were recorded at Gazi University Faculty of Pharmacy using electron ionization (EI) mass spectrometry (Waters-LCT-Premier-XE-LTOF (TOF-MS) instruments; in m/z (rel. %). The liquid chromatography mass spectrometry (LCMS, Waters Micromass ZQ connected with Waters Alliance HPLC (Waters Corporation, Milford, MA, USA), using the ESI (+) method) spectra were recorded at Ankara University Faculty of Pharmacy. The uncorrected melting points were measured using Electrothermal IA9200 apparatus. Absorption spectra were recorded on a Shimadzu 1800 spectrophotometer. Thermal analyses were performed with a Shimadzu DTG-60H system, up to 700 °C (10 °C min^{-1}) under a dynamic nitrogen atmosphere (15 mL min^{-1}).

2.2. Synthesis and characterization of compounds

Carbocyclic amines were diazotized with HCl and $NaNO_2$. A typical reaction condition of diazotizing and coupling is described below using aniline derivatives. The obtained compounds were purified by crystallization using ethanol and then analyzed.

2.3. General synthetic procedures of *I-VI* and *I′-VI′*

2.0 mmol aniline derivative is dissolved in hydrochloric acid (1.5 mL conc. HCl in 4 mL water). The solution was then cooled to 0–5 °C with stirring. Sodium nitrite (0.15 g, 2.0 mmol) in water (3 mL) was gradually added to this solution over 15 min period at 0–5 °C with stirring. The mixture was stirred for an additional 1 h while maintaining at temperature of 0–5 °C. Excess nitrous acid was destroyed by addition of urea. After that, *N*,*N*-diphenylamine or *N*-methyldiphenylamine (2.0 mmol, 0.338 g) was dissolved in acetic acid/propionic acid (4 mL, ratio 3:1) and cooled to 0–5 °C in a salt/ice bath. The cold diazonium salt solution was added to this cooled solution over 1 h with vigorous stirring in a dropwise manner and with the addition of diluted potassium hydroxide solution, pH was mainted in the range of 4–6. The mixture was further stirred for 1 h at 0–5 °C and resulting solid was filtered, washed with cold water and dried in air. The crude product was crystallized by using ethanol.

(E) -1-(4 -((4-(phenylamino)phenyl)diazenyl)phenyl)ethan-1-one (**I**)

Yellow solid; m.p: 184–186 °C; yield: % 80, ^{1}H NMR (DMSO-d_6, 300 MHz): δ_H 9.00 (s, 1H), 8.10 (d, J = 8.54 Hz, 2H), 7.9 (m, 4H), 7.38 (m, 2H), 7.21 (m, 4H), 7.05 (m, 1H), 2.60 (s, 3H) ppm, ^{13}C-APT (DMSO-d_6, 75 MHz): δ_C 197.7; 155.3; 148.7; 145.3; 141.5; 137.5; 129.9; 129.8; 129.5; 125.9; 122.7; 122.4; 120.1; 117.1; 115.1; 27.34 ppm, ^{1}H NMR ($CHCl_3$-d_1, 300 MHz): δ_H 8.11 (q, J = 8.59 Hz, 2H), 7.86 (m, 4H), 7.39 (m, 2H), 7.25 (m, 4H), 7.12 (m, 1H), 6.10 (s, 1H), 2.65 (s, 3H) ppm, HR-MS (ESI, CH_3CN, m/z): $C_{20}H_{18}N_3O$ $[M+H]^+$ found: 316.1450 calcd.: 316.1436.

(E) -(4-((4-(phenylamino)phenyl)diazenyl)benzoic acid (**II**)

Yellow solid; m.p: 246–248 °C; yield: % 50, ^{1}H NMR (DMSO-d_6, 300 MHz): δ_H 9.00 (s, 1H), 8.10 (d, J = 6.81 Hz, 2H), 7.85 (m, 4H), 7.35 (m, 2H), 7.21 (m, 4H), 7.02 (t, J = 7.25 Hz, 1H) ppm, ^{13}C-APT (DMSO-d_6, 75 MHz): δ_C 167.5; 154.9; 148.5; 145.3; 141.5; 133.3; 130.9; 129.8; 125.8; 122.6; 122.2; 120.0; 117.1; 115.2 ppm, HR-MS (ESI, CH_3CN, m/z): $C_{19}H_{15}N_3O_3$ $[M+H]^+$ found: 318.1243 calcd.: 318.1235.

(E) -(4-((4-phenlamino)phenyl)diazenyl)benzonitrile (**III**)

Orange solid; m.p: 186–187 °C; yield: % 75, ^{1}H NMR (DMSO-d_6, 300 MHz): δ_H 9.01 (s, 1H), 8.10 (d, J = 8.64 Hz, 2H), 7.88 (m, 4H), 7.36 (m, 2H), 7.21 (m, 4H), 7.05 (t, J = 7.28 Hz, 1H) ppm, ^{13}C-APT (DMSO-d_6, 75 MHz): δ_C 155.1; 149.2; 145.2; 141.3; 134.1; 129.9; 129,6; 126.2; 123.0; 122.9; 120.3; 120.1; 119.1; 117.1; 115.1; 112.0 ppm, HR-MS (ESI, CH_3CN, m/z): $C_{19}H_{15}N_4$ $[M+H]^+$ found: 299.1302 calcd.: 299.1297.

(E) -4-((4-(nitrophenyl)diazenyl)-*N*-phenylalanine (**IV**)

Dark red solid; m.p: 157–159 °C; yield: %72, ^{1}H NMR (DMSO-d_6, 300 MHz): δ_H 9.02 (s, 1H), 8.45 (d, 2H), 8.00 (m, 4H), 7.45 (m, 2H), 7.30 (m, 4H), 7.12 (t, J = 7.27 Hz, 1H) ppm, ^{13}C-APT (DMSO-d_6, 75 MHz): δ_C 156.4; 149.5; 147.7; 145.3; 141.2; 129.9; 126.5; 125.5; 123.2; 123.1; 120.5; 115.1 ppm, HR-MS (ESI, CH_3CN, m/z): $C_{18}H_{15}N_4O_2$ $[M+H]^+$ found: 319.1194 calcd.: 319.1195.

(E) -4-((4-(chlorophenyl)diazenyl)-*N*-phenylalanine (**V**)

Yellow solid; mp:125–127 °C; yield: %80, ^{1}H NMR (DMSO-d_6, 300 MHz): δ_H 9.00 (s, 1H), 7.82 (m, 4H), 7.61 (d, J = 8.69 Hz, 2H), 7.35 (d, 2H), 7.21 (d, 4H), 7.01 (t, J = 7.27 Hz, 1H) ppm, ^{13}C-APT (DMSO-d_6, 75 MHz): δ_C 151.4; 148.3; 145.1; 141.7; 134.8; 129.8; 125.5; 124.1; 122.5; 121.8; 119.9; 115.3 ppm, HR-MS (ESI, CH_3CN, m/z): $C_{18}H_{15}N_3Cl$ $[M+H]^+$ found: 308.0955 calcd.: 308.0955.

(E) -4-((4-(bromophenyl)diazenyl)-N-phenylalanine (**VI**)

Light orange solid; m.p:150–151 °C; yield: %40, ^{1}H NMR (DMSO-$CDCl_3$-d_1, 300 MHz): δ_H 7.85 (d, J = 8.84 Hz, 2H), 7.77 (d, J = 8.76 Hz, 2H), 7.62 (d, J = 8.76 Hz, 2H) 7.38 (m, 2H), 7.24 (m, 4H), 7.11 (m, 1H), 6.02 (s, 1H) ppm, ^{13}C-APT (DMSO-d_6, 75 MHz): δ_C 151.7; 148.3; 145.1; 141.7; 132.8; 129.8; 125.6; 124.4; 123.6; 122.5; 119.9; 115.3 ppm, HR-MS (ESI, CH_3CN, m/z): $C_{18}H_{15}N_3Br$ $[M+H]^+$ found: 352.0457 calcd.: 352.0449.

(E) -1-(4-((4-(methyl(phenyl)amino)phenyl)diazenyl)phenyl) ethan-1-one (**I′**)

Orange solid; m.p: 142 °C; yield: %49, ^{1}H NMR (DMSO-d_6, 300 MHz): δ_H 8.01 (d, J = 8.59 Hz, 2H), 7.91 (d, J = 8.39 Hz, 2H), 7.83 (d, J = 9.08 Hz, 2H) 7.50 (m, 1H), 7.32 (m, 4H), 6.92 (d, J = 9.11 Hz, 2H), 3.45 (s, 3H) ppm, ^{13}C NMR (DMSO-d_6, 75 MHz): δ_C 155.1; 152.7; 147.1; 144.4; 134.1; 130.5; 126.5; 126.3; 125.8; 123.0; 119.1; 114.6; 111.9 ppm, LC-MS (ESI, CH_3CN): $C_{21}H_{19}N_3O$ $[M+H]^+$ 313.9, HR-MS (ESI, CH_3CN, m/z): $C_{21}H_{19}N_3O$ $[M+H]^+$ 313.1298.

(E) *-2-(4-((4-(methyl(phenyl)amino)phenyl)diazenyl)benzoic acid (**II′**)*

Orange solid; m.p: 241–242 °C; yield: % 49, ^{1}H NMR (DMSO-d_6, 300 MHz): δ_H 13.02, (s, 1H) 8.10 (d, J = 6.77 Hz, 2H), 7.85 (m, 4H) 7.47 (m, 1H) 7.29 (m, 4H), 6.92 (d, J = 9.17 Hz, 2H), 3.45 (s, 3H) ppm, ^{13}C NMR (DMSO-d_6, 75 MHz): δ_C 167.3; 155.3; 152.3; 147.2; 144.6; 131.8; 130.9; 130.4; 126.2; 126.1; 125.8; 125.4; 122.3; 114.8 ppm, HR-MS (ESI, CH_3CN, m/z): $C_{20}H_{18}N_3O_2$ $[M+H]^+$ found: 332.1395 calcd.: 332.1399.

(E) -4-((4-(methyl(phenyl)amino)phenyl)diazenyl)benzonitrile (**III′**)

Orange solid; m.p: 143 °C; yield: % 74, ^{1}H NMR (DMSO-d_6, 300 MHz): δ_H 8.10 (d, J = 8.49 Hz, 2H), 7.85 (m, 4H) 7.47 (m, 1H) 7.29 (m, 4H), 7.10 (d, J = 7.06 Hz, 2H), 3.45 (s, 3H) ppm, ^{13}C NMR (DMSO-d_6, 75 MHz): δ_C 155.1; 152.7; 147.1; 144.4; 134.1; 130.5; 126.4; 125.8; 123.0; 119.1; 114.6; 111.9 ppm, HR-MS (ESI, CH_3CN, m/z): $C_{20}H_{17}N_4$ $[M+H]^+$ found: 313.1459 calcd.: 313.1453.

(E) -N-methyl-4-((4-nitrophenyl)diazenyl)-*N*-phenylalanine (**IV′**)

Dark red; m.p: 170 °C; yield: % 80, ^{1}H NMR (DMSO-d_6, 300 MHz): δ_H 8.37 (d, J = 9.11 Hz, 2H), 7.96 (d, J = 9.92 Hz, 2H), 7.85 (d, J = 9.16 Hz, 2H) 7.50 (m, 1H), 7.32 (m, 4H), 6.91 (d, J = 9.22 Hz, 2H) 3.45 (s, 3H) ppm, ^{13}C NMR (DMSO-d_6, 75 MHz): δ_C 156.4; 152.9; 147.7; 147.0; 144.6; 130.5; 129.7; 126.6; 126.5; 126.0; 125.5; 123.2; 120.5; 114.6 ppm, HR-MS (ESI, CH_3CN, m/z): $C_{19}H_{17}N_4O_2$ $[M+H]^+$ found: 333.1354 calcd.: 333.1352.

(E) -4-((4-chlorophenyl)diazenyl)-*N*-methyl-*N*-phenylaniline (**V′**)

Yellow solid; m.p: 135 °C; yield: % 16, ^{1}H NMR (DMSO-d_6, 300 MHz): δ_H 7.80 (m, 4H), 7.60 (d, J = 8.75 Hz, 2H) 7.45 (m, 1H), 7.26 (m, 4H), 6.96 (d, J = 9.12 Hz, 2H) 3.45 (s, 3H) ppm, ^{13}C NMR (DMSO-d_6, 75 MHz) δ_C 152.0; 151.4; 147.4; 144.4; 134.7; 130.4; 129.8; 126.1; 125.9; 125.1; 124.0; 114.9 ppm, HR-MS (ESI, CH_3CN, m/z): $C_{19}H_{16}ClN_3$ $[M+H]^+$ found: 322.1084 calcd.: 322.1111.

(E) *-4-((4-bromophenyl)diazenyl)-N-methyl-N-phenylaniline (**VI′**)*

Orange solid; m.p: 137 °C; yield: %25, ^{1}H NMR (DMSO-d_6, 300 MHz): δ_H 7.75 (m, 6H), 7.46 (m, 1H) 7.25 (m, 4H) 6.90 (d, J = 9.06 Hz, 2H) 3.45 (s, 3H) ppm, ^{13}C NMR (DMSO- d_6, 75 MHz): δ_C 152.1; 151.7; 147.4; 144.4; 132.8; 130.4; 126.1; 125.9; 125.2; 124.3; 123.5; 114.9, HR-MS (ESI, CH_3CN, m/z): $C_{19}H_{16}BrN_3$ $[M+H]^+$ found: 366.0600 calcd.: 366.0606.

2.4. Computational details

All calculations were carried out using the Density Functional Theory (DFT) approach at the Becke-3-Lee–Yang–Parr (B3LYP) functional [35–37] at 6–31+(G)(d,p) level within the Gaussian 09 program [38]. The ground state of the compounds were obtained in gas phase and various solvents. The confirmation of the convergence to minima on the potential energy surface was made from the vibrational analysis for each molecule. The absorption spectra of the compounds were obtained from TD-DFT calculations at the same level in various solvents. The integral equation formalism of the polarizable continuum model (PCM) [39,40] was employed to evaluate the solvent effects for calculation in solvents. The NLO properties of the compounds were calculated by using finite field method at the same level in gas phase.

3. Results and discussion

3.1. Synthesis and photophysical properties of azo dyes

The azo dyes (**I-VI** and **I′-VI′**) were prepared by coupling Diphenylamine and *N*-Methyldiphenylamine with diazotized some carbocyclic amines having different substituents in hydrochloric acid/water and sodium nitrite (Scheme 1). The synthesized dyes were obtained generally in good yields (91-77%); the structure of these dyes was confirmed by spectroscopic techniques such as ^{1}H/^{13}C NMR and HRMS or LCMS (Supporting Information, Figs. S1-S38).

As seen in Scheme 2, the azo dyes prepared from diphenylamine (**I-VI**) may exist potentially in two tautomeric forms which is named as azo and hydrazone forms. After deprotonation of two tautomers, the common anion is obtained. The UV–vis spectra of the synthesized dyes (**I-VI**) were measured in different solvents with various polarities at a concentration of 3×10^{-5} M. The observed results were compared with their corresponding model dyes (**I′-VI′**). In this study, the dyes synthesized from *N*-methyldiphenylamine (**I′-VI′**) were used as model dyes for determination of stable tautomer of dyes **I-VI**. The photophysical results of dyes in solvents used were given in Table 1. The absorption maxima of all dyes showed bathochromic shifts by increasing polarity of solvents except in proton-donating acetic acid. The λ_{max} values of the all dyes prepared showed the largest bathochromic shifts in highest polar solvent DMSO, as shown in Table 1. However, the dyes **I** and **I′-III′** showed higher λ_{max} values or shoulder in acetic acid while comparing with in DMSO. This result may shown that the formation hydrogen bonds between dye and acetic acid or partial protonation azo group via β-N in azo bridge. The excited state of the dyes may be stabilized by this case (Figs. 1 and 2 and, Figs. S39-S40 in Supporting Information) (see Table 2).

The dyes **I-VI** theoretically may be shown azo-hydrazone tautomers in especially high polar solvents such as DMSO (Scheme 2). For determination of the most stable tautomeric form of the dyes (**I-VI**) in solvents, the model dyes (**I′-VI′**) which are in only azo form in all solvents, were used. While compare λ_{max} values of the both series of dyes, it was observed the dyes (**I-VI**) are stable in azo tautomeric form. However, the small hypsochromic and bathochromic shifts in λ_{max} values of the dyes were observed in these solvents because of solute-solvent interactions.

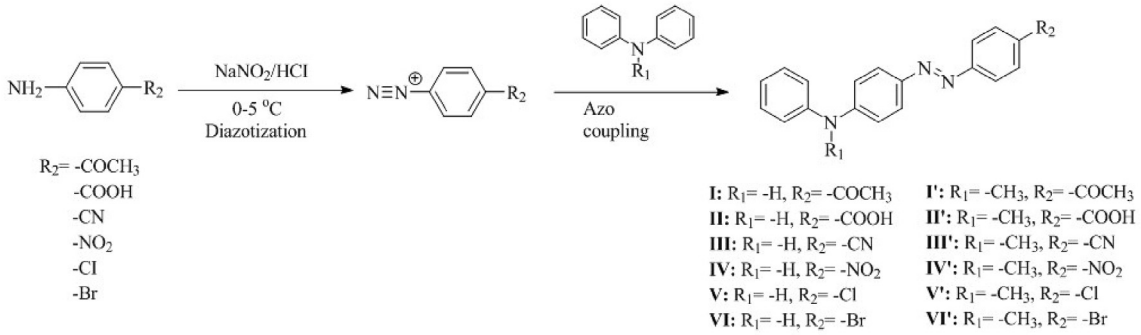

Scheme 1. Synthetic pathway for obtaining of **I-VI** and **I′-VI'**.

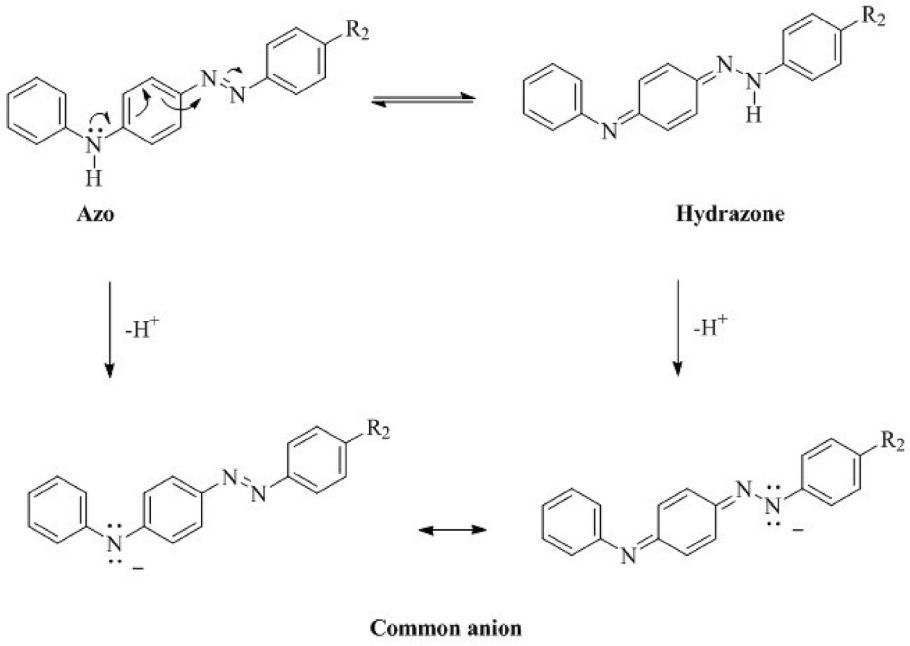

Scheme 2. Possible tautomeric forms and common anion of **I-VI**.

Table 1
The absorption wavelengths (nm) of dyes in various solvents.

Compounds	HOAC	DMSO	DCM	$CHCl_3$	MeOH
I	544	459	432	437.535	443
II	432	439	427	425	432
III	437	464	431	431	444
IV	458	493	452	451	467
V	413	435	409	408	419
VI	414	438	410	409	420
I′	444.551(s)	458	446	446	441
II′	439.550(s)	444	440	439	428
III′	443.553(s)	458	446	446	441
IV′	473	489	476	474	464
V′	416	430	421	419	416
VI′	418	432	423	421	417

s: shoulder.

Table 2
The absorption wavelength values (nm) of the dyes in acidic and basic media in DCM.

Compounds	DCM	DCM + TFA	DCM + Piperidine
I	432	550	432
II	427	541	425
III	431	538	431
IV	452	538	452
V	409	546	409
VI	410	552	410
I′	446	546	446
II′	440	549	440
III′	446	545	446
IV′	464	547	464
V′	421	554	421
VI′	432	552	432

3.2. Substituent effect on absorption spectra of dyes in various solvents

In the push-pull dyes generally include strong donor and acceptor groups in conjugate system.

In this type functional dye, dialkylamino groups use as strong donor, dicyanomethylene, mono/dicyano and nitro groups use as strong acceptor [41].

In our current study, while we choose diphenylamine fragment as strong donor, nitro, cyano etc. groups were choosed as strong

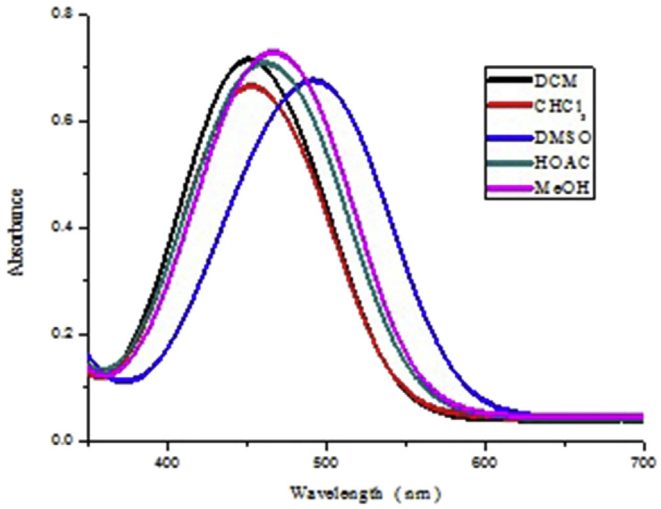

Fig. 1. UV–vis spectra of **IV** in various solvents ($c = 3 \times 10^{-5}$ M).

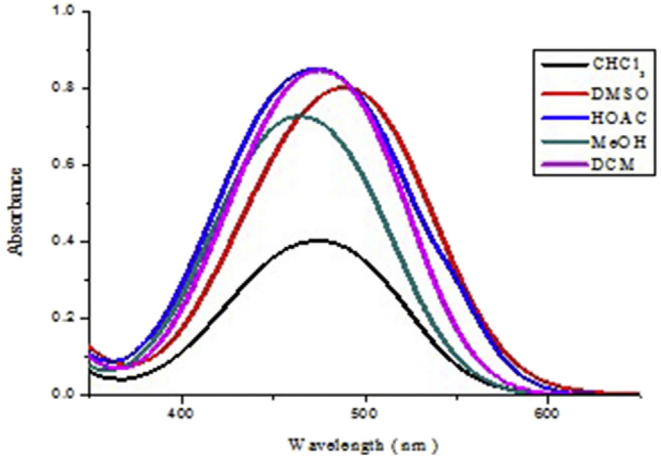

Fig. 2. UV–vis spectra of **IV**′ in various solvents ($c = 3 \times 10^{-5}$ M).

acceptor groups. The UV–Vis spectra of azodiphenylamine dyes bearing electron-accepting and donating substituents are seen in Table 1. While the strong electron-accepting groups such as $-NO_2$, $-CN$ in the para position of the phenyl ring were attached, significant bathochromic shifts were observed in all solvents used. For example, λ_{max} values of dyes for **IV** and **IV'** bearing nitro group were shifted bathochromic in all solvents used relative to other substituents such as $-CN$, $-COOH$, $-COOCH_3$ (for **IV** $\lambda_{max} = 458$ nm bearing NO_2; for **III** $\lambda_{max} = 437$ nm bearing CN). In addition, the λ_{max} values of both series of dyes were seen in longer wavelength in the most polar solvent DMSO relative to other solvents.

3.3. Protonation ability properties

The dyes using as optical pH sensor after protonation (in low pH values) and deprotonation (in high pH values) show various changes of their photophysical properties in absorbance or emission, such as hypsochromic or bathochromic shifts and hyper or hypochromic effects. And they may show color and fluorescence changes that can be seen easily with naked eye. Because of these properties these type dyes can be used optical pH sensor in potential application in clinical and environmental analysis [42].

In this study, the protonation ability of the all dyes in DCM were

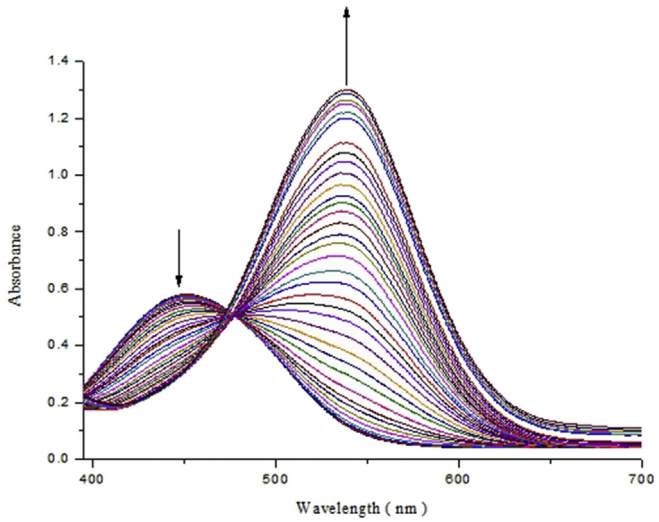

Fig. 3. The absorption spectra of **IV** ($c = 3 \times 10^{-5}$ M) upon addition of TFA (1 M) in DCM.

investigated using TFA as proton source. Upon addition of TFA to a solution of all dyes in DCM, they exhibited clear color changes from yellow to purple with appearing of a new absorption band in long wavelength. For instance, the maximum absorption wavelength of **IV** shift the long wavelength and one isosbestic point located at 485 nm, as a result of the addition of 20 equiv of TFA to **IV** (Supporting Information, Table S1). Upon addition TFA to the solution of all dyes in DCM, β-nitrogen of azo group protonated. The major color changes were observed after protonation from yellow to purple with well-defined isosbestic points at the range of 450–482 nm for the all dyes synthesized (Figs. 3 and 4 and Table S1 in Supporting Information) (Schemes 3 and 4). The obtained the positive charge on β-nitrogen is delocalized in push-pull system of dyes and large bathochromic shift of λ_{max} values with dominant color change for all dyes in comparison with deprotonated form. The obtained red shift after monoprotonation of the azo group can be explained by an increased charge transfer from the diphenylamine/*N*-methyldiphenylamine to the protonated azo group. To

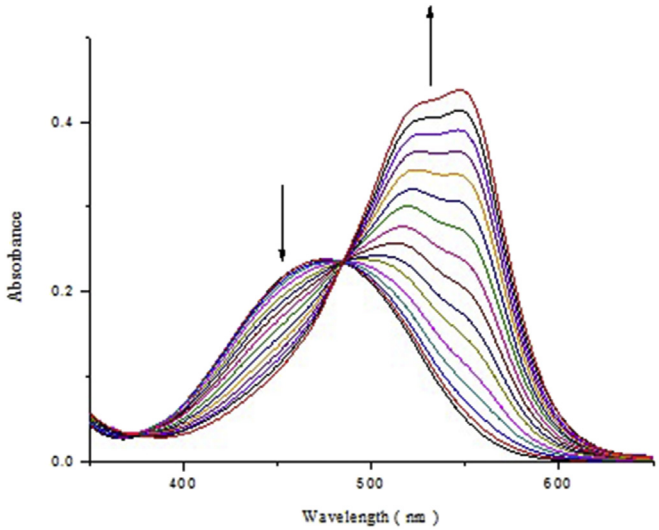

Fig. 4. The absorption spectra of **IV'** ($c = 3 \times 10^{-5}$ M) upon addition of TFA (1 M) in DCM.

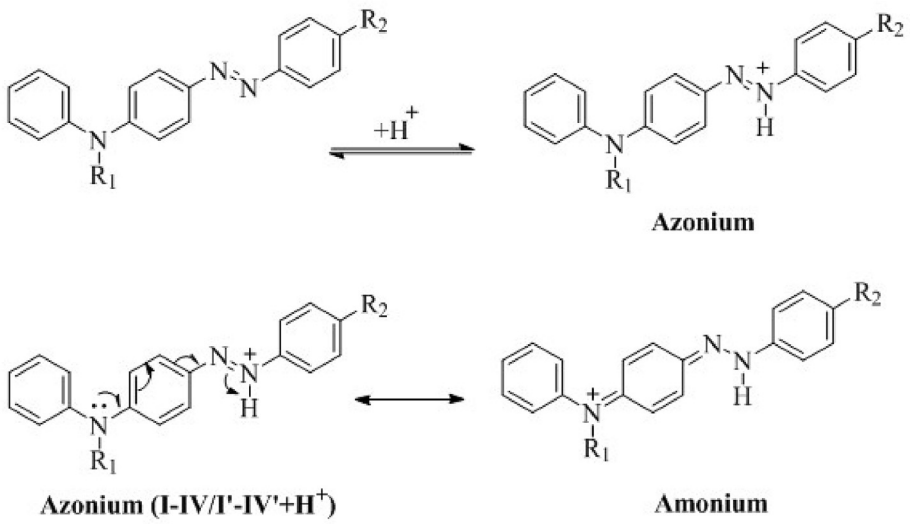

Scheme 3. Protonation of azo group and possible azonium-ammonium forms of dyes.

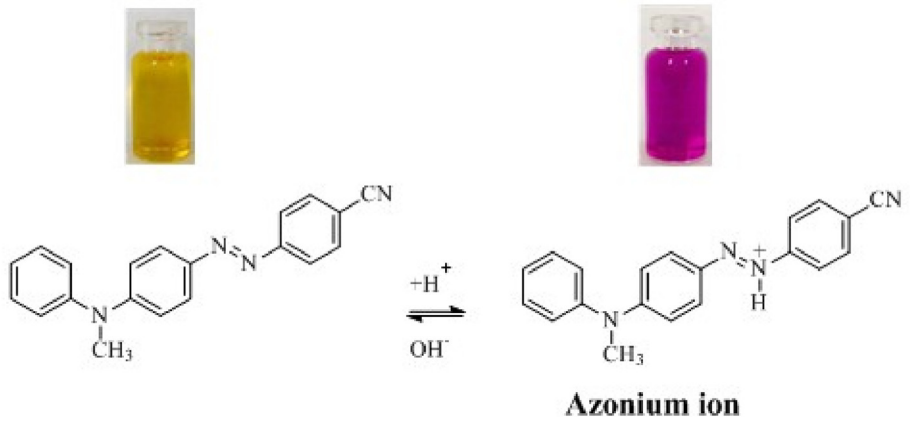

Scheme 4. Color change after protonation of dye **III'**.

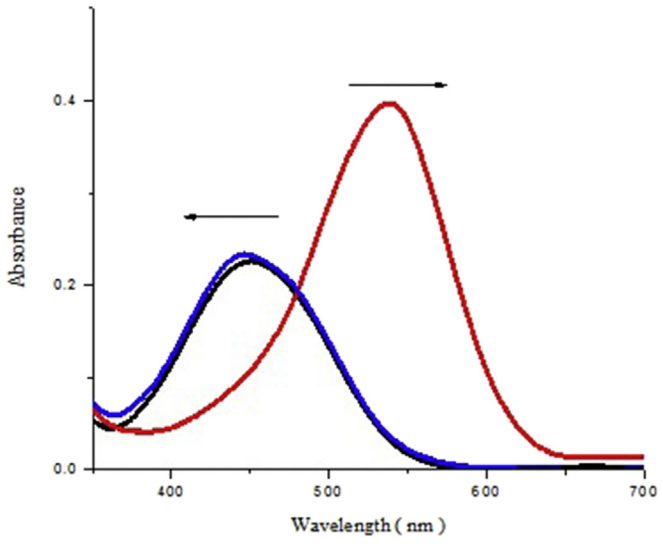

Fig. 5. Absorption spectra of **IV** ($3x10^{-5}$ M) in the absence and presence of TFA and upon addition of piperidine into the acidic DCM (black: **IV**, red: **IV** + TFA, blue: **IV** + TFA + piperidine).

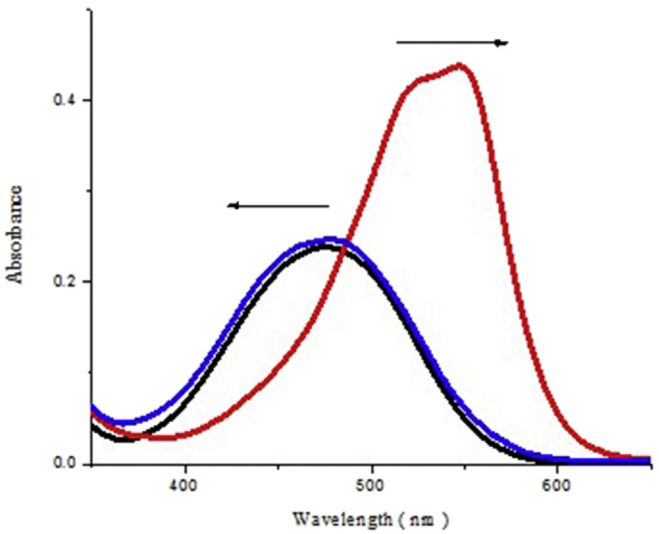

Fig. 6. Absorption spectra of **IV′** **($3x10^{-5}$ M)** in the absence and presence of TFA and upon addition of piperidine into the acidic DCM (black: **IV′**, red: **IV'**+TFA, blue: **IV'**+TFA + piperidine).

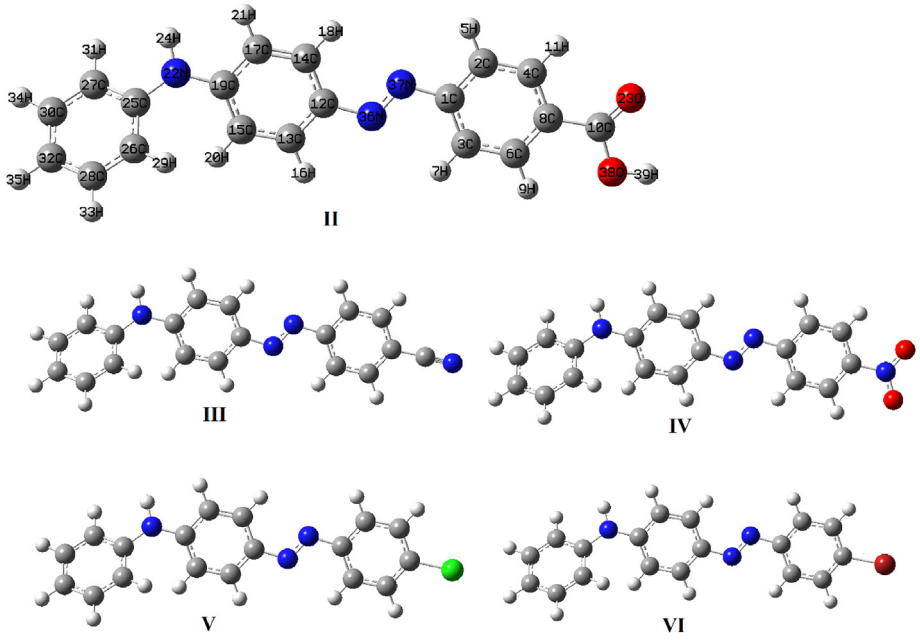

Fig. 7. The optimized geometries of compounds **II-VI**.

Table 3
The total and relative energies (E in a.u, ΔE in kcal/mol) for the azo (*a*) and hydrazone (*h*) forms of **II-VI** in gas phase and different solvents.

			Gas	$CHCl_3$	HOAC	DCM	MeOH	DMSO
II	E	*a*	−1047.81266	−1047.82315	−1047.73063	−1047.82532	−1047.82733	−1047.82758
		h	−1047.79305	−1047.80523	−1047.80654	−1047.80784	−1047.81029	−1047.81060
	ΔE	*a*	0.00	0.00	0.00	0.00	0.00	0.00
		h	12.30	11.24	11.11	10.97	10.69	10.65
III	E	*a*	−951.470865	−951.481298	−951.485609	−951.483414	−951.485369	−951.485609
		h	−951.450045	−951.462769	−951.468327	−951.465473	−951.468012	−951.468327
	ΔE	*a*	0.00	0.00	0.00	0.00	0.00	0.00
		h	13.06	11.63	10.84	11.26	10.89	10.84
IV	E	*a*	−1063.73582	−1063.74642	−1063.74752	−1063.74861	−1063.75065	−1063.75091
		h	−1063.71592	−1063.729	−1063.73043	−1063.73185	−1063.73455	−1063.73488
	ΔE	*a*	0.00	0.00	0.00	0.00	0.00	0.00
		h	12.48	10.93	10.73	10.52	10.10	10.05
V	E	*a*	−1318.82018	−1318.82713	−1318.82789	−1318.82865	−1318.83008	−1318.83026
		h	−1318.79778	−1318.8066	−1318.8076	−1318.8086	−1318.81053	−1318.81078
	ΔE	*a*	0.00	0.00	0.00	0.00	0.00	0.00
		h	14.05	12.88	12.73	12.58	12.27	12.23
VI	E	*a*	−3430.35258	−3430.35954	−3430.36031	−3430.36107	−3430.36251	−3430.36269
		h	−3430.33034	−3430.33917	−3430.34017	−3430.34118	−3430.34311	−3430.34335
	ΔE	*a*	0.00	0.00	0.00	0.00	0.00	0.00
		h	13.96	12.79	12.64	12.48	12.18	12.14

test reversibility property of protonated dyes, same equivalent piperidine was added acidic solution of dyes in DCM. The absorption curve in long wavelength disappeared and a new absorption maximum was observed at shorter wavelength which is same values of absorption maxima of neutral form for all dyes (Figs. 5 and 6 and Figs. S41-S44 in Supporting Information).

3.4. Computational results

The optimized geometries of compounds **II-VI** and **I′-VI′** obtained by performing DFT calculations with B3LYP method and 6−31+g(d,p) basis set. The all data for **I** was taken from Ref. 34, in which compound **I** refers as DPA, for integrity and easy comparison. The obtained geometries and geometry parameters were presented in Fig. 7 Fig. S45 and Table S2-S3 (in Supporting Information). The data of geometry parameters were given in according to the numbering in Fig. 7. The N—N bond length has a double bond character in all structures and a single bond character in hydrazone form of **I-VI**. In all structures, the phenyl and diphenylamine groups are planar along the -N=N- azo bridge. However, the geometrical parameters for azo forms of **I-VI** are compatible with their model dyes (**I′-VI′**).

The stability of the azo and hydrazone forms of **II-VI** were determined with the energy comparison of each compounds. In Table 3, the total and relative energy (E_t and ΔE_t) in gas phase and studied solvents ($CHCl_3$, HOAC, DCM, MeOH and DMSO) were shown for azo and hydrazone forms of each one. As depicted in table, the azo form was more stable than hydrazone form in gas phase and its stability was not affected by solute-solvents interactions. However, it should be noted that the presence of different electron withdrawing group at para position of phenyl ring was not affected the geometrical parameters in two series and

Table 4
The calculated absorption maxima (λ_{max}), oscillator strengths (f) and relevant transitions and CI coefficient for **I-VI** and **I′-VI′** in used solvents. f values are given in parentheses.

	Solvent	λ_{max}, f	Transitions, *CI*		λ_{max}, f	Transitions, *CI*
I [34]	HOAC	471 (1.2857)	H→L, 0.7062	**I′**	482 (1.1981)	H→L, 0.69869
	DMSO	479 (1.3027)	H→L, 0.70554		489 (1.2020)	H→L, 0.69764
	DCM	475 (1.3011)	H→L, 0.70604		485 (0.9595)	H→L, 0.62324
	$CHCl_3$	472 (1.3021)	H→L, 0.70605		482 (1.2187)	H→L, 0.69916
	MeOH	475 (1.2796)	H→L, 0.70604		486 (0.9509)	H→L, 0.62537
II	HOAC	484 (1.1420	H→L, 0.68029	**II′**	477 (1.2063)	H→L, 0.70370
	DMSO	493 (1.2176	H→L, 0.70197		485 (1.0673)	H→L, 0.65938
	DCM	489 (1.0512)	H→L, 0.65133		481 (1.1979)	H→L, 0.69835
	$CHCl_3$	485 (1.1842)	H→L, 0.68683		478 (1.2247)	H→L, 0.70358
	MeOH	489 (1.1605)	H→L, 0.69219		481 (1.1326)	H→L, 0.68670
III	HOAC	484(1.2542)	H→L, 0.70387	**III′**	476 (1.2512)	H→L, 0.70580
	DMSO	492(1.2697)	H→L, 0.70594		483 (1.2110)	H→L, 0.69140
	DCM	488(1.2713)	H→L, 0.70531		480 (1.2626)	H→L, 0.70571
	$CHCl_3$	485 1.2754)	H→L, 0.70400		477 (1.2692)	H→L, 0.70565
	MeOH	488(1.2447)	H→L, 0.70585		479 (1.2381)	H→L, 0.70595
IV	HOAC	553(0.9988)	H→L,0.70692	**IV′**	546 (1.0021)	H→L, 0.70705
	DMSO	569(0.9902)	H→L,0.70718		562 (0.9964)	H→L, 0.70737
	DCM	559 1.0068)	H→L,0.70696		553 (1.0105)	H→L, 0.70715
	$CHCl_3$	551(1.0288)	H→L,0.70670		544 (1.0299)	H→L, 0.70685
	MeOH	564(0.9638)	H→L,0.70725		557 (0.9710)	H→L, 0.70737
V	HOAC	459 (1.2098)	H→L,0.70469	**V′**	452 (1.1660)	H→L, 0.70426
	DMSO	465 (1.2120)	H→L,0.70467		459 (1.0796)	H→L, 0.67598
	DCM	462 (1.1995)	H→L,0.69861		456 (1.1738)	H→L, 0.70371
	$CHCl_3$	459 (1.2311)	H→L,0.70460		453 (1.1850)	H→L, 0.70422
	MeOH	462 (1.1483)	H→L,0.69271		455 (1.1438)	H→L, 0.70270
VI	HOAC	461 (1.2525)	H→L, 0.70430	**VI′**	455 (1.2068)	H→L, 0.70298
	DMSO	467 (1.2551)	H→L, 0.70462		462 (0.8411)	H→L, 0.51526
	DCM	464 (0.8625)	H→L, 0.58154		458 (1.2058)	H→L, 0.69983
	$CHCl_3$	461 (1.2742)	H→L, 0.70425		455 (1.2263)	H→L, 0.70305
	MeOH	464 (1.2224)	H→L, 0.70191		457 (1.1589)	H→L, 0.69367

also stability of azo tautomer of **II-VI**. The same results were reported in Ref. 34 for **I**.

The absorption spectra were calculated using TD-DFT methods at B3LYP/631+g(d,p) level in used solvents. The calculated absorption maxima (λ_{max}), oscillator strength (f) and associated with its orbital contributions were given in Table 4. The substituent effects on absorption spectra were consistent with experimental results. The largest absorption maxima were found for **IV** and **IV′** including strong electron withdrawing group (-NO_2) and the lowest ones were for **V**, **VI** and their model compounds **V′** and **VI′** containing less electron withdrawing groups (i.e. −Br and −Cl). The solvent effects were seen for **IV** and its model compound **IV'** as bathochromic shifted about 18 nm and no significant changes for other compounds from $CHCl_3$ to DMSO. However, the absorption maxima for all studied compounds mainly occurred to the electronic transition from the highest occupied molecular orbital (HOMO) to the lowest unoccupied molecular orbital (LUMO) (Fig. 8 and S46).

To confirm the protonation via α and β nitrogens atom for all compounds in DCM, the protonated forms were optimized and obtained their total and relative energy values were given in Table 5. The comparison of the protonated forms of all compounds confirmed that the β-protonated structure was more stable than the α-protonated structure, so protonation via β nitrogen atom was more likely as depicted in experimental results.

3.5. Non-linear optical (NLO) properties

NLO response of a molecular system containing electron-donor and electron-acceptor units linked through a π-conjugated bridge depends on the conjugated electronic systems, i.e., molecule length and shape as well as the character of donor and acceptor groups. In conjugated organic molecular systems, the reduction of the energy gap between HOMO and LUMO leads to an increase in polarization and NLO response. In addition, dipole moment is an indicator of charge separation within the molecule. In such systems, the large molecular dipole moment, high polarizability and high hyperpolarizability are observed due to donor and acceptor strengths and increasing conjugations.

The quantum chemical calculations by various software packages are often used to predict the efficiency of NLO properties of molecule. In a molecular system, the effects of an applied electromagnetic field are characterized by the polarizabilities (α) and first order hyperpolarizabilities (β). In the calculations, the output provides six compounds of α (αxx, αxy, αyy, αxz, αyz and αzz) and eighteen components of β ijk (i, j, k = x, y and z) and also three compounds of dipol moment (μ_x, μ_y, μ_z). Thus, using the calculation outputs, the dipole moment of a molecule (μ) is defined as follows:

$$\mu = (\mu_x + \mu_y + \mu_z) \quad (1)$$

The average polarizability (α) can be calculated by the following equation:

$$\alpha = 1/3(\alpha_{xx} + \alpha_{yy} + \alpha_{zz}) \quad (2)$$

The magnitude of the static first hyperpolarizability can be calculated using the following equations:

$$\beta_{tot} = (\beta^2{}_x + \beta^2{}_y + \beta^2{}_z) \quad (3)$$

where,

$$\beta_x = (\beta_{xxx} + \beta_{xyy} + \beta_{xzz}) \quad (4)$$

$$\beta_y = (\beta_{yyy} + \beta_{xxy} + \beta_{yzz}) \quad (5)$$

$$\beta_z = (\beta_{zzz} + \beta_{xzz} + \beta_{yzz}) \quad (6)$$

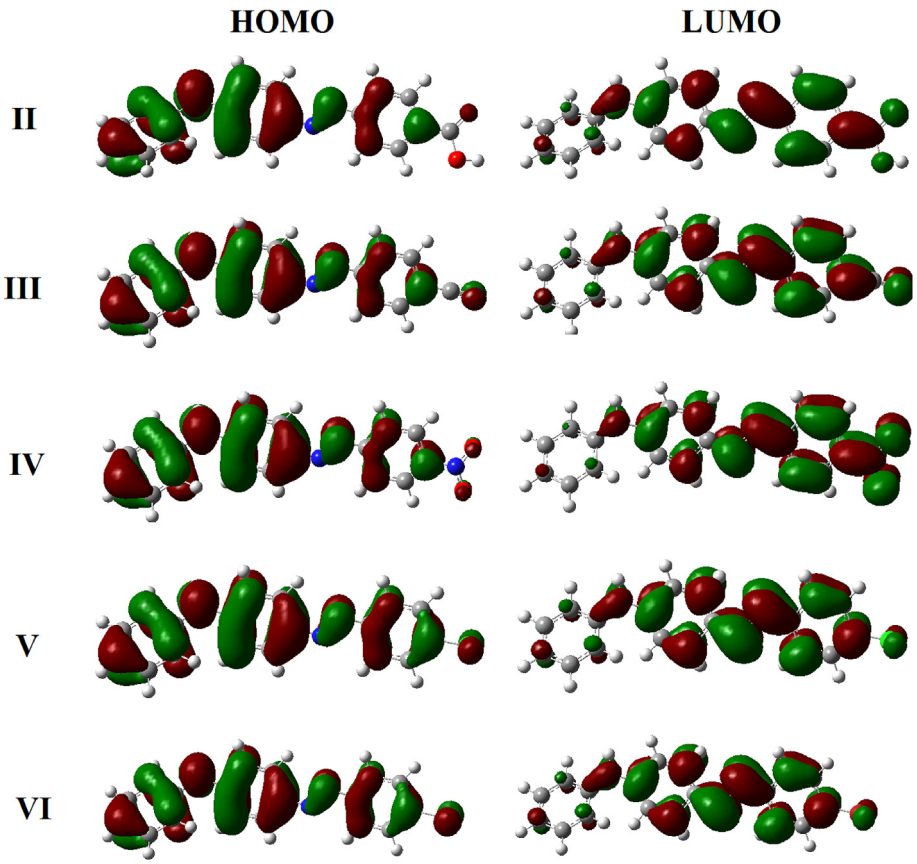

Fig. 8. The frontier orbitals of **II-VI.**

The obtained values of μ, α and β from Eqs. (1)–(6) and their components obtained from the calculation output are listed in Table 6 and Table S4. The largest dipole moment was 10.13 D and 11.56 D for **IV** and its model compound **IV′** due to the presence of $-NO_2$ group when the compared with the other compounds. In case of **V/VI** and **V'/VI′** including the weakest electron-acceptor −Cl and −Br, the dipole moment was the smallest one as 4.65 D and 6.03–6.05 D, respectively. Similarly, the presence of the strong electron-accepting group decreased the energy gap between HOMO and LUMO for **IV** and **IV'** (Table 7). Thus, the hyperpolarizability values were observed as the largest value $\beta = 270.4 \times 10^{-30}$ esu for **IV** and $\beta = 239.8 \times 10^{-30}$ esu for **IV′** and the smallest values $\beta = 86.7 \times 10^{-30}$ esu for **V**, $\beta = 89.9 \times 10^{-30}$ esu for **VI** and $\beta = 69.9 \times 10^{-30}$ esu for **V′**, $\beta = 73.1 \times 10^{-30}$ esu for **VI'**. Also, the comparison of β values of the studied compounds with the value of prototype molecule urea ($\beta = 0.38 \times 10^{-30}$ esu) shows that compounds have higher values than urea as 230–720 times for **I-IV**, 186–639 times for **I′-VI'**. From these results, it can be concluded that these compounds may be recommended for future NLO studies.

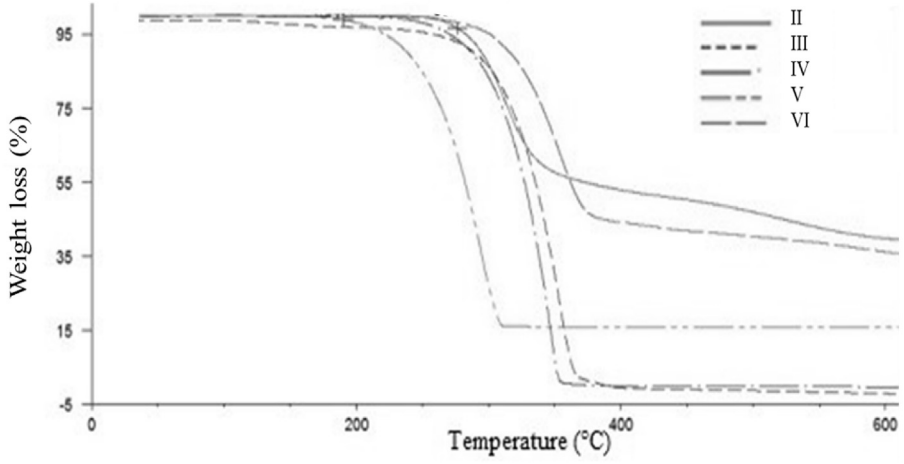

Fig. 9. TGA curves of **II-VI**.

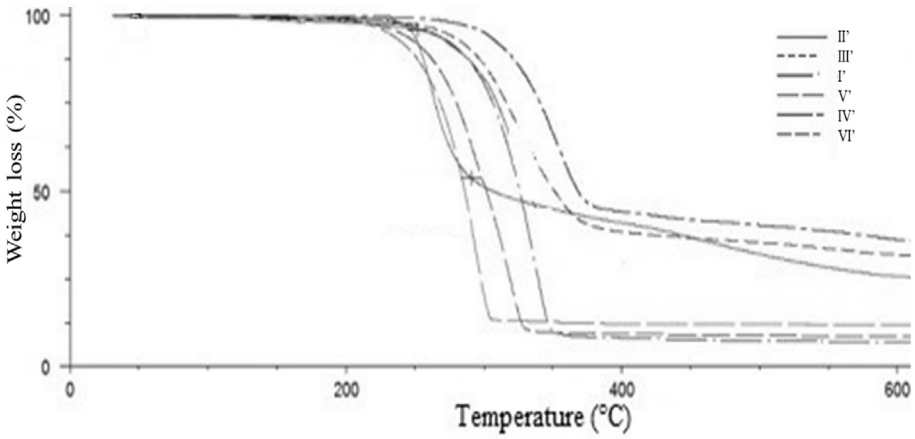

Fig. 10. TGA curves of **I′-VI′**.

Table 5
Total energy and relative energy values of the protonated **I-VI** and **I′-VI′** via α and β nitrogens atom in DCM.

		E (a.u)	ΔE (kcal/mol)			E (a.u)	ΔE (kcal/mol)
I	α	−1012.320732	5.67	**I′**	α	−1051.626359	5.94
	β	−1012.329766	0.00		β	−1051.63582	0.00
II	α	−1048.2516375	5.78	**II′**	α	−1087.557375	5.98
	β	−1048.2608409	0.00		β	−1087.566902	0.00
III	α	−951.9079033	5.90	**III′**	α	−991.213668	6.14
	β	−951.917298	0.00		β	−991.22345	0.00
IV	α	−1064.171183	6.36	**IV′**	α	−1103.477065	6.59
	β	−1064.181324	0.00		β	−1103.48757	0.00
V	α	−1319.257229	4.57	**V′**	α	−1358.56266	4.89
	β	−1319.264506	0.00		β	−1358.570448	0.00
VI	α	−3430.789672	4.61	**VI′**	α	−3470.095064	4.93
	β	−3430.797021	0.00		β	−3470.102916	0.00

3.6. Thermal characterization

The determination of thermal property of dyes is very important for their usability in electro optic materials. To determine the thermal stability of the all synthesized dyes, thermogravimetric analysis (TGA) was used. The change in weight of the compounds was measured as a function of temperature. Thermal stability of the dyes is shown in Figs. 9 and 10 and S47-S48 (in Supporting Information). The absence of weight loss in the range of 0–100 °C indicates that the solids have no water molecule. The initial

Table 6
The electric dipole moment (μ), the polarizability (α) and the first hyperpolarizability (β_{tot}) and their components calculated at the B3LYP/6−31+g(d) level in gas phase for **II-VI**. The components are in a.u.

	II	III	IV	V	VI
μ_x	−2.240265	−3.5100455	−3.9228564	−1.7732323	−1.7841925
μ_y	−0.103851	0.712242	0.7061897	0.4419206	0.4056969
μ_z	−0.1244186	0.0117641	0.0027141	−0.0122946	−0.0162391
μ (D)	**5.71**	**9.10**	**10.13**	**4.65**	**4.65**
α_{xx}	687.9063553	700.2876797	717.3529512	645.9534372	673.490449
α_{xy}	9.7716061	−3.3590893	4.5433864	4.2425266	9.2826867
α_{yy}	234.8155804	224.8876855	235.3579422	224.7463849	230.2223446
α_{xz}	10.6368353	9.5805577	10.314842	9.7373303	9.8932406
α_{yz}	0.1349964	0.7319935	0.7257733	1.272439	0.9590457
α_{zz}	141.7226519	139.6625451	139.1882058	139.6522411	145.4654532
α (x10^{-24}) esu	**52.6**	**52.6**	**53.9**	**49.9**	**51.8**
β_{xxx}	20506.60706	18897.80037	31695.49868	10347.99727	10679.14287
β_{xxy}	−1004.05995	−1067.492224	−1905.616902	−429.19933	−230.5849848
β_{xyy}	−366.2875454	−296.3945059	−327.4595435	−258.6161253	−266.6068514
β_{yyy}	35.7059622	37.9067562	55.1323719	8.1333901	−11.1401944
β_{xxz}	−48.6285327	−93.4413814	−127.8017402	−46.0716367	−43.2126488
β_{xyz}	−45.5815701	−38.8077455	−51.1717838	−16.951617	−28.1880899
β_{yyz}	−14.4866225	−18.163339	−15.7054165	−20.7693166	−19.6526534
β_{xzz}	−94.8141671	−92.3695529	−125.0026333	−62.6655028	−13.7111023
β_{yzz}	−11.2704899	−1.3008396	1.8416816	−7.3431915	−15.2871649
β_{zzz}	−11.1734596	−6.0117274	−6.6821093	−4.0113568	−6.0364116
β_{tot} (x10^{-30}) esu	**173.4**	**160.2**	**270.4**	**86.7**	**89.9**

Table 7
The energy gap between HOMO and LUMO (ΔE) and the energies of HOMO and LUMO (E_{HOMO} and E_{LUMO}) for **I-IV** and **I′-IV′**.

	I	II	III	IV	V	VI
E_{HOMO} (a.u)	−0.20911	−0.20963	−0.21355	−0.21674	−0.20558	−0.20564
E_{LUMO} (a.u)	−0.09989	−0.09973	−0.10441	−0.11602	−0.09043	−0.09091
ΔE (eV)	2.97	2.99	2.97	2.74	3.13	3.12
	I′	**II′**	**III′**	**IV′**	**V′**	**VI′**
E_{HOMO} (a.u)	−0.20568	−0.20624	−0.21027	−0.21364	−0.20202	−0.20207
E_{LUMO} (a.u)	−0.09555	−0.09528	−0.09983	−0.11216	−0.08561	−0.08611
ΔE (eV)	3.00	3.02	3.01	2.76	3.17	3.16

decomposition temperatures (T_d) of dyes showed that the dyes have enough thermal stability while using as optic dyes in electro optic (EO) material [43].

4. Conclusions

In summary, two series of azo dyes were prepared by coupling diphenylamine and *N*-methyl diphenylamine and diazotized substituted anilines bearing various substituents. The compounds were characterized by spectroscopic techniques such as $^{1}H/^{13}C$ NMR and HRMS or LCMS. Photophysical properties were investigated by experimentally and theoretically in various solvents with different polarity. The absorption maxima were observed in longer wavelength in the most polar solvents DMSO. In addition, the most stable tautomeric form of compounds (**I-VI**) were determined using model compounds (**I′-VI′**) which are stable only in azo form. The results showed that the compounds (**I-VI**) are stable in azo form.

The structural and electronic properties, stabilities of tautomeric structures and NLO properties of **II-VI** were obtained within the computational calculations by DFT methods. The same analysis were done their model compounds to compare the obtained data. The comparison of energy stabilities calculations showed that the azo form is dominant in gas phase and studied solvents. The calculation results were in accordance with experimental data. Moreover, it is obtained that the compounds have a high NLO response in gas phase: the first hyperpolarizability of **I-IV** (**I′-VI′**) were higher than urea as 230–720 (186–639) times. The both compounds series are thermally stable and T_d values are bigger than 220 °C. Therefore, they can be offered as potential candidates for NLO applications.

Declaration of competing interest

The authors declare that they have no known competing financial interests or personal relationships that could have appeared to influence the work reported in this paper.

CRediT authorship contribution statement

Tuğçe Aksungur: Conceptualization, Investigation, Writing - original draft. **Fatma Erol:** Conceptualization, Investigation. **Nurgül Seferoğlu:** Conceptualization, Software, Writing - review & editing. **Zeynel Seferoğlu:** Conceptualization, Methodology, Writing - review & editing.

Acknowledgements

The authors are grateful to Prof. Dr. Gülsen Asman for giving us use to their UV–Vis spectrometer in Gazi University Department of Chemistry. The numerical calculations reported in this paper were fully performed at TUBITAK ULAKBIM, High Performance and Grid Computing Center (TRUBA resources).

Appendix A. Supplementary data

Supplementary data to this article can be found online at https://doi.org/10.1016/j.molstruc.2020.128449.

References

[1] P.F. Gordon, P. Gregory, Organic Chemistry in Color, Springer- Verlag, Berlin Heidelberg, 1983.
[2] Y. Do Kim, J.H. Cho, C.R. Park, J.H. Choi, C. Yoon, J. P. Synthesis Kim, Application and investigation of structure–thermal stability relationships of thermally stable water-soluble azo naphthalene dyes for LCD red color filters, Dyes Pigments 89 (1) (2011) 1–8.
[3] H. Zollinger, Color Chemistry: Syntheses, Properties, and Applications of Organic Dyes and Pigments, John Wiley & Sons, 2003.
[4] H. Zollinger, Diazo chemistry II, Aliphatic. Inorg. Organomet. Compd. 1 (1995) 522.
[5] H. Horiguchi, Gousei Senryou, Synthetic Dyes, Sankyo Shuppan, Tokyo, 1969.
[6] S. Abeta, K. Imada, Kaisetsu Senryou Kagaku, Dye Chemistry, Shikisensya, Osaka, 1989.
[7] H.A. Lubs, The Chemistry of Synthetic Dyes and Pigments, Hafner Publishing, New York, 1965.
[8] P. Gregory, High-technology Applications of Organic Colorants, Prenum Press, New York, 1991.
[9] D.R. Waring, G. Hallas, The Chemistry and Application of Dyes, Plenum Press, New York, 1990.
[10] M. Matsuoka, Infrared Absorbing Dyes, Plenum Press, New York, 1990.
[11] A.D. Towns, Developments in azo disperse dyes derived from heterocyclic diazo components, Dyes Pigments 42 (1) (1999) 3–28.
[12] E. Marchevsky, R. Olsina, C. Marone, 2-[2-(5-Chloropyridyl)azo]-5-(dimethylamino) phenol as indicator for the complexometric determination of zinc, Talanta 32 (1) (1985) 54–56.
[13] S. Manickasundaram, P. Kannan, Q.M.A. Hassan, P.K. Palanisamy, Azo dye based poly(alkyloxymethacrylate)s and their spacer effect on optical data storage, J. Mater. Sci. Mater. Electron. 19 (11) (2008) 1045–1053.
[14] M.M.M. Raposo, A.M.C. Fonseca, M.C.R. Castro, M. Belsley, M.F.S. Cardoso, L.M. Carvalho, et al., Synthesis and characterization of novel diazenes bearing pyrrole, thiophene and thiazole heterocycles as efficient photochromic and nonlinear optical (NLO) materials, Dyes Pigments 91 (1) (2011) 62–73.
[15] D. El Mekkawi, M.S.A. Abdel-Mottaleb, The interaction and photostability of some xanthenes and selected azo sensitizing dyes with TiO2 nanoparticles, Int. J. Photoenergy 7 (2) (2005) 95–101.
[16] G.I. Nosova, I.G. Abramov, N.A. Solovskaya, N.N. Smirnov, E.V. Zhukova, V.B. Lyskov, et al., Synthesis and photophysical properties of soluble polyimides and polyquinazolones containing side-chain chalcones or azo chromophores, Polym. Sci. B 53 (1–2) (2011) 73–88.
[17] A.C. Razus, L. Birzan, M. Cristea, V. Tecuceanu, L. Blanariu, C. Enache, Novel monoand bis- azo dyes containing the azulen-1-yl moiety, synthesis, characterization, electronic spectra and basicity, Dyes Pigments 80 (3) (2009) 337–342.
[18] M. Panda, N.D. Paul, S. Joy, C.H. Hung, S. Goswami, Hydrido iridium(III) complexes of azoaromatic ligands, isolation, structure and studies of their physicochemical properties, Inorg. Chim. Acta. 372 (1) (2011) 168–174.
[19] J. Koh, A.J. Greaves, Synthesis and application of an alkali-clearable azo disperse dye containing a fluorosulfonyl group and analysis of its alkali-hydrolysiskinetics, Dyes Pigments 50 (2001) 117–126.
[20] R. Vijayaraghavan, N. Vedaraman, M. Surianarayanan, D.R. MacFarlane, Extraction and recovery of azo dyes into an ionic liquid, Talanta 69 (5) (2006) 1059–1062.
[21] S. Machida, M. Araki, K. Matsuo, Studies of the water-soluble polymers, XVI. Azo dyes of poly-N-vinylimidazole, J. Appl. Polym. Sci. 12 (2) (1968) 325–332.
[22] W.G. George, Dyes and liquid crystals, Dyes Pigments 3 (1982) 203–209.
[23] K. Nejati, Z. Rezvani, M. Seyedahmadian, The synthesis, characterization, thermal and optical properties of copper, nickel, and vanadyl complexes derived from azo dyes, Dyes Pigments 83 (3) (2009) 304–311.
[24] J. Zyss, Molecular Nonlinear Optics, Materials, Physics and Devices, Academic Press, Boston, MA, USA, 1994.
[25] Jin-An He, B. Shaoping, L. Lian, Jayant Kumar, K. Tripathy Sukant, A. Samuelson

Lynne, Photochemical behavior and formation of surface relief grating on self-assembled polyion/dye composite film, J. Phys. Chem. B 104 (2000) 10513–10521.
[26] W. Lin, W. Lin, G.K. Wong, T.J. Marks, Supramolecular approaches to sec-ondorder nonlinear optical materials, Self-assembly and microstructural characterization of intrinsically acentric [(aminophenyl) azo] pyridinium superlattices, 7863, 1996, pp. 8034–8042.
[27] X. Wang, J. Kumar, S.K. Tripathy, L. Li, J. Chen, S. Marturunkakul, Epoxy-based nonlinear optical polymers from post azo coupling reaction, Macromolecules 30 (1997) 219–225.
[28] G. Arunmozhi, E.de M. Gomes, S. Ganesamoorthy, Growth kinetics of zinc (tris) thiourea sulphate (ZTS) crystals, Crystal Research and Technology, J. Exp. Ind. Crystallogr. 39 (5) (2004) 408–413.
[29] M. Lawrence, J. Thomas Joseph Prakash, Spectrochim. Acta, Part A 91 (2012) 30–34.
[30] P.M. Ushasree, R. Jayavel, C. Subramanian, P. Ramasamy, Growth of zinc thiourea sulfate (ZTS) single crystals, a potential semiorganic NLO material, J. Cryst. Growth 197 (1–2) (1999) 216–220.
[31] H.S. Nalwa, S. Miyata, Non-Linear Optics of Organic Molecules and Polymers, CRC Press, Boca Raton, FL, USA, 1997.
[32] E. Vogel, Technology and metrology of new electronic materials and devices, Nat. Nanotechnol. 2 (1) (2007) 25–32.
[33] A. Diaspro, G. Chirico, M. Collini, Two-photon fluorescence excitation and related techniques in biological microscopy, Q. Rev. Biophys. 38 (2006) 97–166.
[34] T. Aksungur, O. Arslan, N. Seferoğlu, Z. Seferoğlu, Photophysical and theo-retical studies on newly synthesized N,N-diphenylamine based azo dye, J. Mol. Struct. 1099 (2015) 543–550.
[35] A.D. Becke, J. Chem. Phys. 8 (1993) 5648–5652.
[36] C.T. Lee, W. Yang, R.G. Parr, Phys. Rev. B 37 (1988) 785–789.
[37] P.J. Stephens, F.J. Devlin, C.F. Chabalowski, M.J. Frisch, J. Phys. Chem, 98 (2994) 11623-11627.
[38] M.J. Frisch, G.W. Trucks, H.B. Schlegel, G.E. Scuseria, M.A. Robb, J.R. Cheeseman, G. Scalmani, V. Barone, B. Mennucci, G.A. Petersson, H. Nakatsuji, M. Caricato, X. Li, H.P. Hratchian, A.F. Izmaylov, J. Bloino, G. Zheng, J.L. Sonnenberg, M. Hada, M. Ehara, K. Toyota, R. Fukuda, J. Hasegawa, M. Ishida, T. Nakajima, Y. Honda, O. Kitao, H. Nakai, T. Vreven, J.A. Montgomery Jr., J.E. Peralta, F. Ogliaro, M. Bearpark, J.J. Heyd, E. Brothers, K.N. Kudin, V.N. Staroverov, T. Keith, R. Kobayashi, J. Normand, K. Raghavachari, A. Rendell, J.C. Burant, S.S. Iyengar, J. Tomasi, M. Cossi, N. Rega, J.M. Millam, M. Klene, J.E. Knox, J.B. Cross, V. Bakken, C. Adamo, J. Jaramillo, R. Gomperts, R.E. Stratmann, O. Yazyev, A.J. Austin, R. Cammi, C. Pomelli, J.W. Ochterski, R.L. Martin, K. Morokuma, V.G. Zakrzewski, G.A. Voth, P. Salvador, J.J. Dannenberg, S. Dapprich, A.D. Daniels, O. Farkas, J.B. Foresman, J.V. Ortiz, J. Cioslowski, D.J. Fox, Gaussian 09, Revision C.01, Gaussian, Inc., Wallingford CT, 2010.
[39] R. Bauernschmitt, R. Ahlrichs, Treatment of electronic excitations within the adiabatic approximation of time dependent density functional theory, Chem. Phys. Lett. 256 (1996) 454–464.
[40] M. Cossi, V. Barone, Time-dependent density functional theory for molecules in liquid solutions, J. Chem. Phys. 115 (2001) 4708–4717.
[41] (a) Virendra R. Mishra, Chaitannya W. Ghanavatkar, Nagaiyan Sekar, ESIPT clubbed azo dyes as deep red emitting fluorescent molecular rotors, Photo-physical properties, pH study, viscosity sensitivity, and DFT studies, J. Lumin. 215 (2019), 116689;
(b) M.M. Raikwar, E. Mathew, M. Varghese, I.H. Joe, N. Sekar, NLOphoric tri-phenylamine derived donor-p-acceptor-p-donor based colorants: synthesis, spectroscopic, density functional theory and Z-scan studies, Photochem. Photobiol. 95 (2019) 931–945.
[42] (a) A. Bergen, A. Granzhan, H. Ihmels, Photochem. Photobiol. Sci. vol. 7 (2008) 405, 407;
(b) S. Achelle, J. Rodriguez-Lopez, F.J. Robin-le Guen, Org. Chem. 79 (2014) 7564–7571;
(c) S. Achelle, A. Barsella, C. Baudequin, B. Caro, F. Robin-le Guen, J. Org. Chem. 77 (2012) 4087–4096;
(d) C. Hadad, S. Achelle, J.C. García-Martinez, J. Rodríguez-Lopez, J. Org. Chem. 76 (2011) 3837–3845;
(e) S. Achelle, S. Kahlal, J.Y. Saillard, N. Cabon, B. Caro, F. Robin-le Guen, Tet-rahedron 70 (2014) 2804–2815.
[43] G. Deng, H. Xu, H. Huang, J. Jiang, J. Kun, X. Zhang, Z. Li, J. Liu, Synthesis and properties study of a novel nonlinear optical chromophore containing benzo [b]furan moiety based on julolidine, J. Mol. Struct. 1196 (2019) 439–443.